The Role of $^1\pi\sigma^*$ States in the Formation of Adenine Radical-Cations in DNA Duplexes

Tolga N. V. Karsili[†, *], Barbara Marchetti[‡, ¥] and Michael N. R. Ashfold[¥, *]

[†]*Department of Chemistry, University of Louisiana, Lafayette, LA 70504, USA*

[‡]*Department of Chemistry, University of Pennsylvania, Philadelphia, PA 19128, USA*

[¥]*School of Chemistry, University of Bristol, Bristol, BS8 1TS, UK*

*Corresponding authors' contact details

Tolga.karsili@louisiana.edu

Mike.ashfold@bristol.ac.uk

Article intended for issue celebrating Wolfgang Domcke's 70th birthday

Abstract

Photoinduced damage of DNA is a well-known but still far from fully understood phenomenon. Electronic structure methods are here employed to investigate potential roles of $\pi\sigma^*$ states in initiating photodamage, and ways in which $\pi\sigma^*$-state driven photochemistry might evolve with increasing molecular complexity. The study starts with the bare 9H-adenine molecule and progresses through to a model double-helix DNA duplex in aqueous solution. Relative to the gas phase, aqueous solvation is predicted to stabilize the $^1\pi\sigma^*$ states of these systems when exciting at the respective ground state equilibrium geometries, but to have relatively little effect on the asymptotic N–H bond strengths. But the study also re-emphasises the potential importance of rival $\sigma^* \leftarrow \pi$ excitations, wherein a solute π electron is promoted to a σ^* orbital localized on an O–H bond of a complexing H_2O molecule, as a route to forming parent radical cations – as have recently been observed following near UV photoexcitation of double-helix adenine-thymine duplexes in water (Banyasz *et al*., *Farad. Disc*. **207**, 181 (2018)). The subsequent deprotonation of such radical cations offers a rival low energy route to N–H bond fission and radical formation in such duplexes.

1. Introduction

The role of πσ* excited states in molecular photochemistry has attracted much attention over the past two decades.[1–4] Such states are ubiquitous in heteroaromatic and heteroatom (X) containing cyclic molecules such as (thio)phenols,[5–11] indoles [12,13] and pyrroles,[14–16] as well as their biological analogues – *e.g.* adenine,[17–19] thymine/uracil,[20,21] and guanine.[22] In all such molecules, near-ultraviolet (UV) electronic excitation can result in direct or indirect (*via* non-adiabatic coupling) population of πσ* states, *i.e.* states formed by electron promotion from a valence π or non-bonding *n* orbital to an unoccupied σ* orbital that is localized around the acidic X–H bond. Population of the σ* orbital inevitably lowers the X–H bond order, thus manifesting in the characteristically dissociative nature of such πσ* states with respect to X–H bond extension.

The dominant process following near-UV excitation of pyrrole or imidazole is N–H bond fission, yielding pyrrolyl (imidazolyl) + H products.[14,15,23,24] N–H bond fission occurs directly after photoexcitation to the ^{1}πσ* state, which is the lowest singlet excited electronic state (*i.e.* the S_1 state) in both molecules. The excited-state dynamics of (thio)phenols are similarly dominated by πσ* state mediated (S)O–H bond fission but, in these cases, the πσ* continuum may be populated by internal conversion (IC) from the pre-excited (bright) ^{1}ππ* (S_1) state, which is the dominant contributor to the respective near- UV absorption spectra.[7,12]

Excitations to ring-centered ^{1}ππ* states similarly dominate the UV absorption spectrum of indole (a bicyclic heteroaromatic molecule with a higher density of π and π* orbitals than pyrrole or (thio)phenol).[25,26] The first two excited singlet states of indole are both of ππ* character. In contrast to pyrrole and (thio)phenol, excitation to the lower of these two ^{1}ππ* states (the S_1 state, traditionally known as the L_b state) populates a long-lived ($\tau > 5$ ns) excited state that displays no evidence of X–H (in this case N–H) bond fission. The second ^{1}ππ* state (the L_a state) shows a ~4-fold stronger absorption cross section than the L_b state and is populated at excitation wavelengths, $\lambda < 273$ nm. Population of the L_a state is followed by non-adiabatic coupling with, and subsequent internal conversion to, the ^{1}πσ* continuum and some formation of indolyl + H products at shorter excitation wavelengths ($\lambda < 263$ nm).[12,13]

Adenine is another bicyclic heteroaromatic molecule with a near-UV absorption spectrum that is dominated by excitations to the first two ^{1}ππ* states.[27] As with indole, N–H bond fission is

observed at short excitation wavelengths ($\lambda < 233$ nm in this case) and attributed to dissociation following non-adiabatic coupling to the $\pi\sigma^*$ state.[18] In contrast to indole, however, adenine molecules excited to either of these $^1\pi\pi^*$ states decay on an ultrafast (~300 fs) timescale, by IC to the S_0 state.[28 , 29] This decay is driven by out-of-plane ring-bending motions centered on the six-membered component of this bicyclic molecule.[30–32]

Such out-of-plane ring-bending distortions are now recognized as nuclear motions that can access regions of degeneracy between excited state potential energy surfaces (PESs), or between the ground and excited state PESs in conjugated cyclic molecules. When motions orthogonal to the ring-bending distortions are considered, these degeneracies develop into conical intersections (CIs) that are now understood to mediate many of the ultrafast processes observed in molecular photochemistry.[33,34] CIs play a pivotal role in facilitating the dissipation of electronic excitation in the DNA/RNA nucleobases, nucleosides and nucleotides, and the associated oligonucleotides and base pairs, enabling efficient reformation of the ground-state molecule. Such photostability is exhibited by many biologically relevant molecules.[35,36] Many recent experimental and theoretical studies have explored the mechanisms that confer photostability in biologically relevant molecules – such as those found in the mammalian epidermis.[37] Such molecules contain specific functions that are intended to absorb and to dissipate UV-radiation incident upon the human body – thereby offering greater protection to cellular DNA.

Notwithstanding, cellular DNA damage may occur upon prolonged UV exposure. Such damage can occur when cellular imbalances encourage rival photochemical processes to become competitive with the non-radiative IC processes that promote photostability. These alternative photochemical paths may lead to the irreversible formation of photoproducts.[38–41] Near UV-induced cycloaddition reactions are responsible for one common family of DNA photoproducts – the cyclobutane pyrimidine dimer (CPD) adducts formed when neighboring nucleobases on a common strand undergo cycloaddition reactions. Oxidative DNA damage is another common photoreaction. Recent experimental studies have succeeded in detecting radical-cation precursors to such oxidation products in single stranded naked DNA,[42] in DNA duplexes [43] and in Guanine-rich G-quadruplexes.[44] Photoexcitation studies of a model adenine-thymine DNA duplex and a G-quadruplex at $\lambda \leq 266$ nm return (low) quantum yields for forming the respective radical cations (*i.e.* the species formed by electron loss from the parent) and solvated electrons,

and detect the radical species formed by subsequent deprotonation of the radical cation.[43,44] Complementary electronic structure calculations suggest that the deprotonation step involves cleavage of a (non-hydrogen bonded) N–H bond in the terminal amino-group on a single adenine or guanine molecule, in, respectively, the duplex DNA and the model G-quadruplex, but the mechanism of the initial electron ejection following absorption of such low energy photons remains unclear.

Here we explore the extent to which such radical cations could arise *via* πσ* state driven photochemistry, focusing particularly on the (non-hydrogen bonded) N–H bond of the amino group of adenine in a model DNA duplex. Our hypothesis builds on the known characteristics of πσ* states, their propensity to facilitate X–H bond fission in isolated gas phase molecules, and the ways in which such behavior is modified when the solute of interest is in aqueous solution. Phenol provides a good example. πσ* state mediated O–H bond fission in the isolated molecule has been extensively studied, both experimentally and theoretically,[5,6,8,10,11,45–47] and recent ultrafast time-resolved studies following near-UV excitation of phenol in aqueous solution have revealed spectral signatures of both phenoxyl radicals and solvated electrons.[48,49] Such findings accord with the earlier theoretical predictions by Domcke and Sobolewski, who showed that the πσ* state of phenol is stabilized when bound to a small cluster of water molecules.[45] In contrast to the isolated phenol molecule, the πσ* state of the phenol-water cluster is formed by promoting an electron from a phenol-centred π-orbital to a σ*-orbital centred on an O–H bond of a complexing H_2O molecule. This represents a much longer-range charge separation than that achieved by σ*←π excitation in bare phenol. Here we explore the possible roles of πσ* states in forming potentially damaging radical-cations following near-UV photoexcitation of double-helix adenine-thymine duplexes in aqueous solution. A systematic 'bottom-up' approach is adopted, wherein electronic structure methods are used to investigate the near-UV photochemistry of, first, isolated 9H-adenine molecules (henceforth abbreviated as Ade) and then progressively extrapolated to the bulk double-helix DNA duplexes.

2. Computational Methodology

Using Gaussian 09,[50] the ground state equilibrium geometries of all neutral and cationic systems were optimized using the long-range corrected ωB97XD [51] functional of Density Functional Theory (DFT), coupled to the 6-31G(d) Pople basis set.[52] Isolated 9H-adenine and the 9H-adenine-1H-thymine base pair were optimized both as isolated gas phase systems and with a polarization continuum model, using a water solvent and a dielectric constant of 78.35. Vertical excitation energies of gas phase 9H-adenine were calculated both at the time dependent (TD) DFT/ωB97XD/6-31G(d) level and with complete active space with second-order perturbation theory (CASPT2). The latter was coupled to an aug-cc-pVDZ basis set and based on a state-averaged complete active space self-consistent field (SA7-CASSCF) reference wavefunction, across the lowest seven singlet states. An active space of 10 electrons in 10 orbitals (the *n*2p, three π, three π*, 3s Rydberg, σ and σ* orbitals) was used as well as an imaginary level shift of 0.5 E_H. The CASSCF/CASPT2 oscillator strengths were calculated using equation (1):

$$f = \frac{2}{3}\left(E_j - E_i\right) \cdot \sum_{\alpha=x,y,z} \left|\mu_{ij}\right|_{\alpha}^{2} \qquad (1)$$

where E_j and E_i are the CASPT2 energies of the final (i.e. S_1, S_2, S_3 or S_4) and initial (S_0) states, respectively, and μ_{ij} are the transition dipole moments accompanying a given $i \rightarrow j$ transition, along α (α = *x*, *y* and *z* coordinates).

Mixed quantum and classical mechanics computations were carried out for adenosine, the deoxyadenosine-deoxythymidine base pair and a model (deoxyadenosine-deoxythymidine)(deoxythymine-deoxyadenosine) duplex solvated in a TIP3P truncated octahedral box of solvent water molecules. These calculations used the ONIOM [53] interfacial model implemented in Gaussian 09. In ONIOM, different molecular components of an ensemble are sub-divided into layers, which are treated at different computational levels and the total energy calculated on a subtractive basis. In our present systems, the high layer comprised the DNA nucleobase(s) and was computed at the DFT/ωB97XD/6-31G(d) level of theory. The medium layer was calculated using the semi-empirical PM6 method [54] and comprised the ribose-phosphate backbone and K^+ counter ions. The low layer was computed using AMBER [55] molecular mechanics force-field theory and comprised the entire system. The duplex configuration was prepared using the NUCLEIC program as implemented in AmberTools.[56] Once prepared and neutralized with K^+ counterions, the resulting structure was solvated using PACKMOL.[57]

The corresponding radicals formed by N–H bond fission were computed for all the systems and in the same environment as the closed-shell parent structures from which they derive. The reported relative radical energies (E_{rel}) are referenced to that of the adeninyl radical formed by N9–H bond fission in an isolated gas phase adenine molecule and calculated as per eq. (2):

$$E_{rel} = \left(E_{radical} - E_{parent}\right) - \Delta E_{9H-adenine} \quad (2)$$

where $\Delta E_{9H-adenine} = \left(E_{radical\ (adenine(-9H))} - E_{parent\ (9H-adenine)}\right)$.

The bond dissociation energies (BDEs) are then calculated using eq. (3):

$$BDE = D_0(\mathrm{N9-H}) + E_{rel} \quad (3)$$

where D_0(N9-H) is the experimental bond dissociation energy of gas-phase 9H-adenine.

Vertical ionization energies were computed for all systems, from the minimum energy geometry of the respective ground-state neutral species. Adiabatic ionization energies were derived by optimizing the +1 cation for all but the DNA duplex (for which we were unable to converge the ground state minimum energy geometry).

3. Results and Discussion

The molecular structures explored in this work are shown in Figure 1, which also serves as a 'road map' for the ensuing narrative. The heavy atom labels in (a) will be used when discussing the photochemistry of Ade and extended as required when describing Ade in more complex environments. Table 1 lists the relative stabilities of the radical co-fragments formed by N6'–H and (where possible) N9–H bond fission in each case. These E_{rel} values are the calculated energy differences between the parent molecule and the radical formed by loss of the indicated H atom, in the specified local environment, and are quoted relative to the calculated endothermicity of N9–H bond fission in the bare adenine molecule (eq. (1)). Negative values thus indicate dissociation processes that are calculated to be less endoergic than N9–H bond fission in bare adenine. The

bond dissociation energies (BDEs) listed in the final column of Table 1 are estimated simply by shifting the documented N9–H BDE of gas phase adenine [18] by the appropriate calculated energy difference. We recognize that these reported values (particularly those in aqueous solution) are likely to be over-estimates of the 'true' BDE, since the present calculations will not recognize any solvent induced stabilization of the open-shell H-atom partner.

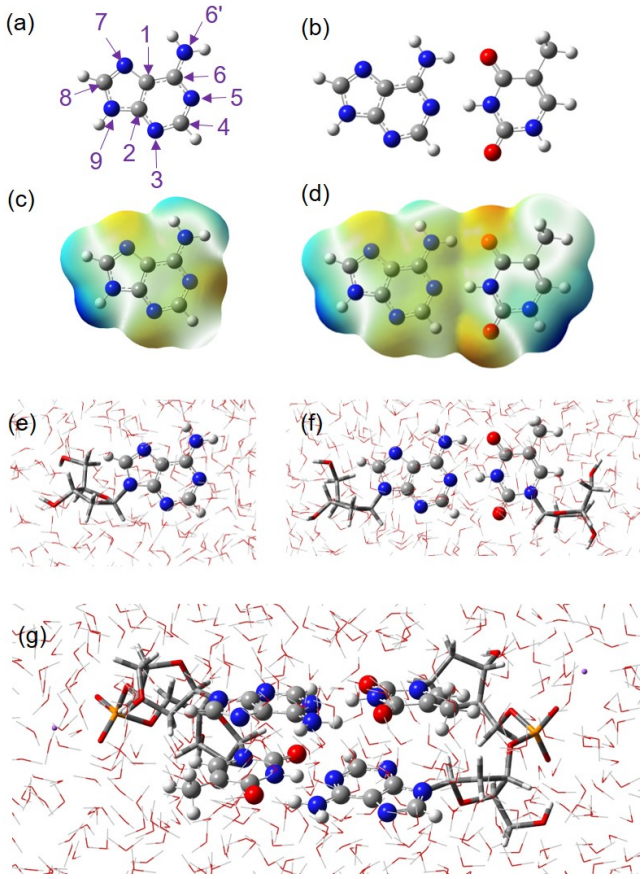

Figure 1: Optimized ground state geometries of (a) 9H-adenine and (b) the adenine-thymine base pair in the isolated gas phase, the same base (c) and base pair (d) in a polarization continuum model (PCM) and (e) adenosine, (f) deoxyadenosine-deoxythymidine and (g) a (deoxyadenosine-deoxythymidine)(deoxythymine-deoxyadenosine) duplex in aqueous solution.

Adenine in the gas phase

We start by reprising the documented excited states and excited state dynamics of Ade, the optimised ground (S_0) state geometry of which was shown in Figure 1(a). The first four singlet excited states at this equilibrium geometry are of $n\pi^*$, $\pi\pi^*(L_b)$, $\pi\pi^*(L_a)$ and $\pi\sigma^*$ character, respectively. Figure 2 depicts the orbitals, orbital promotions, energies (and oscillator strengths) associated with these various excitations. As shown, the $S_1 \leftarrow S_0$ transition has a low oscillator strength, reflecting the poor spatial overlap between the initial (n) and final (π^*) orbitals, whereas the $S_2 \leftarrow S_0$ (particularly) and $S_3 \leftarrow S_0$ transitions have higher oscillator strengths, consistent with the improved overlap between the participating π and π^* orbitals.

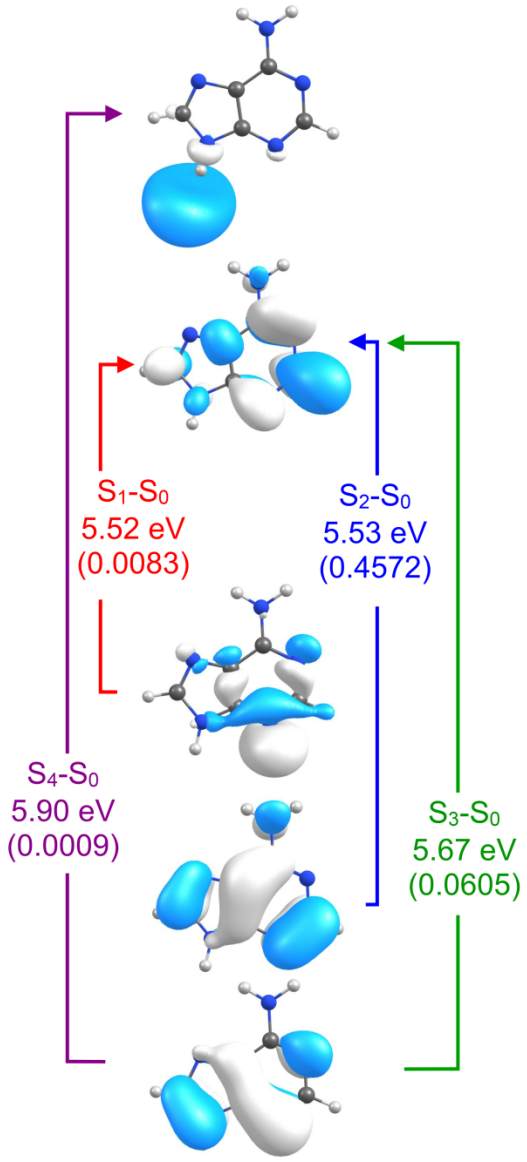

Figure 2: CASSCF Orbitals and dominant orbital promotions associated with electronic excitations to the first four excited singlet states of Ade. The calculated CASPT2 vertical excitation energy is given alongside each transition, as well as the oscillator strength (in parentheses).

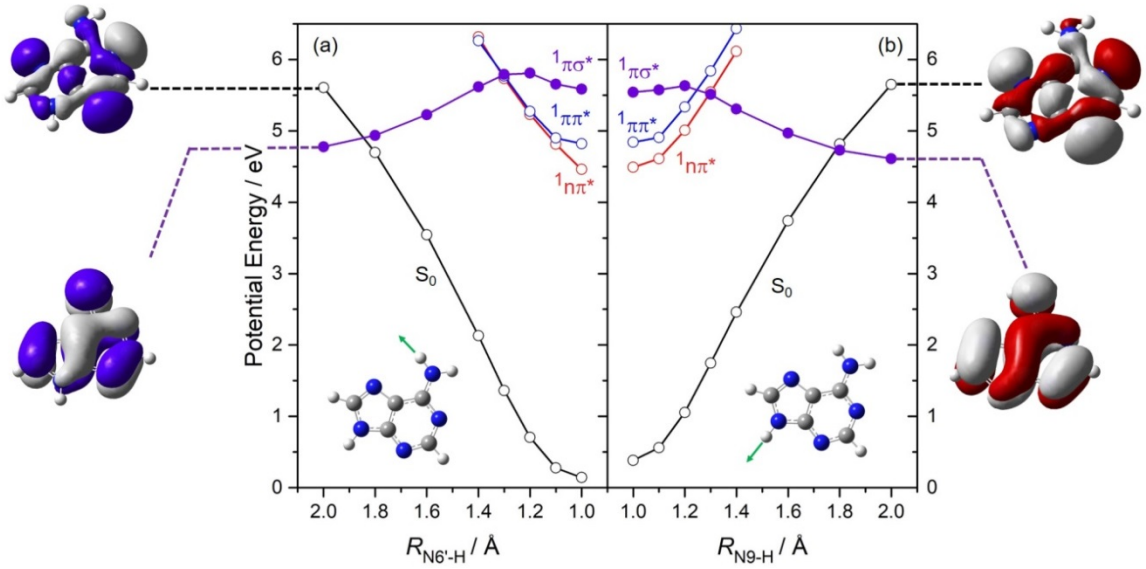

Fig. 3: CASPT2 calculated potential energy profiles for gas phase 9H-adenine molecules along the $R_{N9–H}$ and $R_{N6'–H}$ coordinates, adapted from reference [32]. In these computations the N–H bond was varied, and the remainder of the nuclear framework allowed to relax to the minimum energy configuration of the $^1\pi\sigma^*$ state (filled purple circles). The remaining electronic states were computed at the corresponding relaxed $^1\pi\sigma^*$ state geometry. The $2^1\pi\pi^*$ state PE profile has been omitted in order to avoid cluttering the figure.

Figure 3 shows PE profiles (adapted from reference [32]) for the S_0, S_1, S_2 and S_4 states of Ade along the N9–H and N6'–H bond extension coordinates ($R_{N9–H}$ and $R_{N6'–H}$) calculated at the relaxed geometry of the $S_4(^1\pi\sigma^*)$ state. The corresponding profiles for the $S_3(L_a)$ state are very similar to those of the $S_2(L_b)$ state and have been omitted to avoid cluttering the figure. The ground, $n\pi^*$ and $\pi\pi^*$ (L_b and L_a) states are each bound along both $R_{N9–H}$ and $R_{N6'–H}$, whereas the $^1\pi\sigma^*$ state is dissociative with respect to extending either N–H bond. The 'shelf' in this PE curve around the Franck-Condon (FC) region arises as a result of mixing between the diabatic $^1\pi3s$ Rydberg and $^1\pi\sigma^*$ pure-valence states. In the high-symmetry limit, both states transform to a common anti-symmetric irreducible representation which leads to a same-symmetry avoided crossing.[58] The topography of the $^1\pi\sigma^*$ state is thus determined by the lower adiabat returned from this avoided crossing. The extent to which the $^1\pi3s$ Rydberg state and the $^1\pi\sigma^*$ valence state couple depends

on the energetic disposition of the two diabatic states, the former of which (in the Koopmans' limit) has a predictable quantum defect with respect to the ground state cation (*vide infra*).

As Figure 3 also shows, the $^1\pi\sigma^*$ state correlates diabatically with H + ground state adeninyl radical fragments (henceforth represented as Ade(-*n*H), where *n* is the numerical label of the de-hydrogenated N atom). The singly occupied molecular orbital (SOMO) in the ground state Ade(-9H) and Ade(-6'H) radicals (*i.e.* the radicals formed by, respectively, parent N9–H or N6'–H bond fission) is a ring-centered $p\pi$-orbital – illustrated at the relevant asymptote in figure 3. In this configuration, the in-plane N-centered $p\sigma$-orbital is doubly occupied and thus inevitably displays a long-range repulsive interaction with an H(^{2}S) atom approaching in the molecular plane, which ultimately constitutes the $^1\pi\sigma^*$ state at the vertical geometry. The odd-electron in the first excited states of both the Ade(-9H) and Ade(-6'H) radicals, in contrast, is in the SOMO-1 orbital (*i.e.* in the upper orbital depicted in figure 3). These SOMO-1 orbitals are both localized in the molecular plane and, as in many similar heteroatom containing systems,[1] it is the first excited state of the Ade(-9H) and the Ade(-6'H) radical that exhibits a long-range attractive interaction and correlates diabatically with the S_0 state parent molecule upon decreasing $R_{N–H}$.

Translationally excited H atom products have been reported following near-UV excitation of gas phase adenine at $\lambda \leq 233$ nm, consistent with one-photon induced dissociation on the $^1\pi\sigma^*$ PE surface and formation of Ade(-*n*H) + H products. Analysis of the deduced total kinetic energy release spectrum of the products returned an N–H bond strength of 34580 ± 50 cm^{-1} (4.29 ± 0.01 eV) and the vibrational energy disposal in the Ade(-*n*H) products was shown to be consistent with N9–H bond fission.[18] Such a conclusion matches expectations based on the PE profiles shown in Figure 3, and with the relative stabilities of the radical products listed in Table 1.

Adenine and adenosine in aqueous solution

Table 1 also shows that the effective N9–H and N6'–H BDEs are both reduced by implicit water solvation (PCM), reflecting some stabilization of the Ade(-9H) and Ade(-6'H) radicals by solvation with a polar molecule. The ionization potential of Ade in implicit water solvation is also predicted to decrease. Coupled with the decrease in BDE, this is a strong indicator that the entire $^1\pi\sigma^*$ state potential is stabilized by solvation with water molecules.

The ionization potential and N6'–H BDE for adenosine in an explicit water solvent (ONIOM) are also both calculated to be lower than the corresponding quantities in bare adenine. Again, the SOMO in the ground state radical formed by N–H bond fission is the ring-centered $p\pi$-orbital (see fig. S1 of the ESI), implying that the in-plane $p\sigma$-orbital, local to the N6' atom, is doubly occupied and that interaction with this orbital is responsible for the long-range repulsive region of a $^1\pi\sigma^*$ state upon decreasing $R_{N6'\text{-}H}$.

Adenine-thymine base pair in the gas phase and in aqueous solution

Upon pairing with 1H-thymine (henceforth Thy), the resulting H-bonded Ade-Thy base pair has a greater excited state density and its near-UV absorption shows a bathochromic shift *cf.* bare Ade or Thy.[59] The long wavelength excitations are to locally excited states (*i.e.* the orbitals involved in the electronic transition are localised on one nucleobase). Charge transfer states, involving electron exchange between the Ade and Thy orbitals, are predicted to lie at higher vertical energies.[59]

As Table 1 shows, Ade-Thy base pairing is predicted to reduce the ionization potential (*cf.* Ade) and to leave a non-hydrogen-bonded N6'–H bond that could – at least in principle – be susceptible to near-UV photoinduced bond fission. The quantum yield for any such photodamage will be limited by the ultrafast rate of IC to the S_0 state, which is dominated by electron-driven proton-transfer between the Ade and Thy nucleobases.[59] Nevertheless, Table 1 predicts only a small increase in the endoergicity of N6'–H bond fission in gas-phase Ade-Thy (*cf.* N9–H bond fission in isolated Ade), suggesting that prolonged UV-exposure of the Ade-Thy base pair might induce N–H bond fission. This modest destabilization of the radical when paired with Thy can be

attributed to the weakening of the remaining (hydrogen-bonded) N–H bond by the reduced electronegativity of the amino-group centered N-atom.

Notwithstanding this modest destabilization, the SOMO of the ground state Ade(-6'H)-Thy radical still retains $p\pi$-character (see fig. S1 of ESI) implying that, again, the N6'-centred $p\sigma$-orbital is doubly occupied and will inevitably induce a long-range repulsive interaction with an incident H atom – which, again, will constitute a $\pi\sigma^*$ state of the parent base pair as $R_{N6'-H}$ is reduced. Implicit solvation stabilizes the Ade(-6'H)-Thy radical (see Table 1), though we note that these radicals are predicted to be marginally less stable than the solvated Ade(-6'H) radicals. As with Ade, solvation of Ade-Thy is also predicted to (substantially) reduce the adiabatic ionization energy (*cf.* the isolated base pair), implying an energetic lowering of the $^1\pi3s$ Rydberg state in the Franck-Condon region and thus of the mixed Rydberg-valence $^1\pi\sigma*$ state.

Table 1: Calculated (non-zero-point corrected) parent ionization energies, (relative) radical stabilities and associated parent N–H bond dissociation energies (in eV). All gas phase (GAS) and PCM computations employed the ωB97XD/6-31G(d) level of theory, while the ONIOM computations used ωB97XD/6-31G(d) for the high-layer, PM6 for the medium layer and AMBER for the low-layer, as described in the Methodology section.

Molecule	**Parent Adiabatic Ionization Energy**	**Bond**	**Radical product energy (E_{rel}) relative to that of Ade(-9H)**	**Effective BDE referenced to the N9–H bond strength in gas phase adenine**
Adenine (GAS)	7.89	N9–H	0	4.29
Adenine (GAS)	7.89	N6'–H	0.12	4.41
Adenine-Thymine (GAS)	7.56	N6'–H	0.18	4.47
Adenine (PCM)	6.00	N9–H	–0.04	4.25
Adenine (PCM)	6.00	N6'–H	0.05	4.33

Adenine-Thymine (PCM)	5.99	N6'–H	0.15	4.44
Adenosine (ONIOM)	6.99	N6'–H	–0.10	4.19
Deoxyadenosine-Deoxythymidine (ONIOM)	6.94	N6'–H	0.07	4.36
Deoxyadenosine-Deoxythymidine Duplex (ONIOM)	5.78‡	N6'–H	0.16	4.45

‡Value is the calculated vertical ionization energy and thus represents an upper limit to the adiabatic ionization energy.

Deoxyadenosine-Deoxythymidine and a Deoxyadenosine-Deoxythymidine Duplex in aqueous solution

Extending to the more complex DNA-duplex (fig. 1(g)) leads to obvious changes in the electronic absorption spectrum when compared with the isolated gas-phase Ade molecule. We caution that the absorption spectra in Figure 4 have been derived using the lowest 10 vertically excited energies and that the energies returned by TDDFT methods will almost inevitably be upper bounds to the true excitation energies. By way of illustration, the first absorption maximum in the near UV absorption spectrum of adenine is observed at ~250 nm,[60] and the origin of the $\pi\pi^*(L_b)\leftarrow S_0$ transition lies at ~275 nm,[61] so the primary purpose of figure 4 is to give a qualitative comparison of the likely absorption of this DNA-duplex in an aqueous environment relative to that of gas-phase Ade. As fig. 4 shows, the higher density of π and π^* orbitals in duplex-DNA manifests itself as a broader absorption, with greater intensity at long wavelengths (*cf*. isolated Ade). The latter is likely to encourage enhanced absorption probability to the various locally excited states and to the excitonic states in duplex-DNA (*cf*. to the corresponding states in isolated Ade and the Ade-Thy base pair).

N6'–H bond fission in either of the adenosine molecules within the duplex yields a radical (henceforth dAde(-6'H)-dThy~dThy-dAde) that is calculated to be 0.16 eV less stable that Ade(-

9H). This implies a slightly larger N6'–H BDE in the duplex when compared to the N9–H BDE of Ade. Although dAde(-6'H)-dThy~dThy-dAde is less stable than Ade(-9H), the destabilization is such that the relevant energies still lie well within the near-UV wavelength range required to access the asymptote for forming dAde(-6'H)-dThy~dThy-dAde + H products. Yet again, the SOMO in the radical associated with the lowest energy dissociation asymptote of dAde(-6'H)-dThy~dThy-dAde is a π-orbital (shown in fig. S1 of the ESI), implying that the in-plane N-centred *p*σ-orbital is doubly occupied and will show a repulsive interaction with an incident H atom – manifesting in the long-range part of the $^1\pi\sigma^*$ state PE surface. The vertical ionization energy in the duplex environment is lower than in any other system studied, implying a large stabilization of the $^1\pi\sigma^*$ state potential at vertical FC geometries. Thus we conclude that the dAde(-6'H)-dThy~dThy-dAde radical could also arise as a result of dissociation via a $^1\pi\sigma^*$ state. In addition, we have computed the electron affinity of a $(H_2O)_{40}$ cluster solvated in a continuum model of bulk water at the same level of theory as the above calculations. The returned adiabatic electron affinity of the $(H_2O)_{40}$ cluster is 0.2 eV which, when subtracted from the vertical ionization energy of dAde(-6'H)-dThy~dThy-dAde, indirectly implies a charge-separated state at ~5.58 eV.

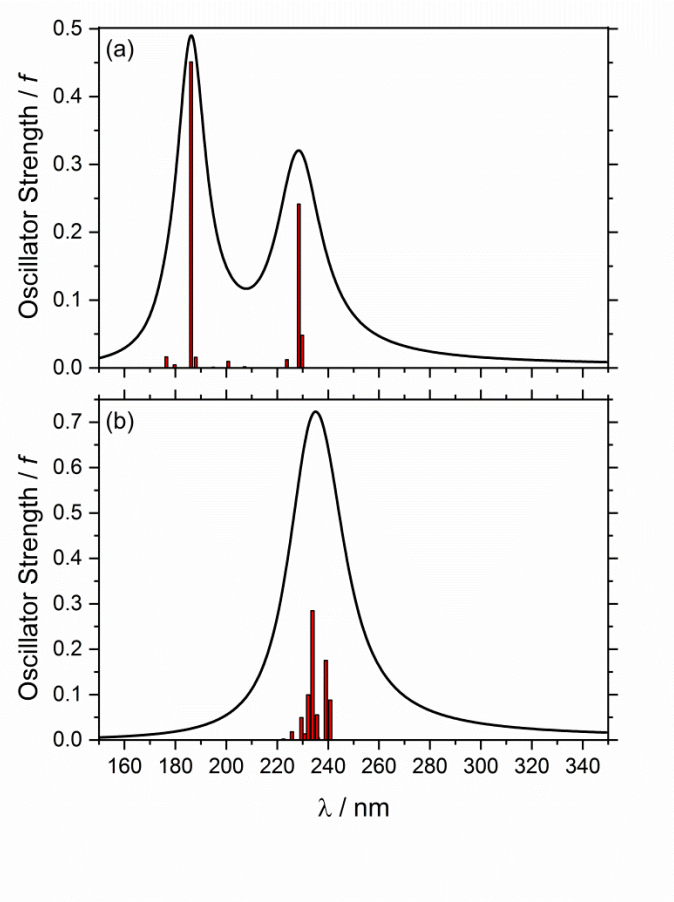

Fig. 4: Simulated absorption spectra of (a) isolated 9H-adenine in the gas phase and (b) double-helix duplex DNA in aqueous solution. Computations used the TD-DFT/ωB97XD/6-31+G(d) level of theory. A sum (over 10 lowest excited states) of Lorentzian line shape functions, each with a 0.5 eV (FWHM) broadening factor, was used to simulate the overall spectral profile.

4. General Discussion and Conclusions

A systematic bottom-up approach has been used to explore the energetic feasibility of $^1\pi\sigma^*$ state driven N–H bond fission in systems ranging from bare adenine through to duplex double-helix DNA in aqueous solution. Recent experiments by Markovitsi and co-workers have identified a (minor) channel leading to parent radical-cations following near-UV excitation of duplex DNA in aqueous solution.[43] Guided by electronic-structure calculations, these authors deduced that radical-cation (plus solvated electron) formation is followed by proton loss from one of the non-hydrogen-bonded N6′–H bonds, thereby restoring local charge neutrality. The parent radical-

cation and/or the radical formed upon subsequent deprotonation were then shown to undergo a series of side-reactions leading to, predominantly, a cycloadduct.

These authors left open the possible parent radical-cation formation mechanism at such low photon energies. Here we highlight the possibility that their formation (and subsequent N–H bond fission) is mediated by πσ* excited states. Such states are ubiquitous in heteroaromatic molecules, and the present work starts by illustrating their role in enabling N–H bond fission in isolated adenine and adenosine molecules and in Ade-Thy base pairs. This conclusion is largely driven by the occupancy of the SOMO and SOMO-1 orbitals of the resulting radical, and the energies and geometries of the ground state radical and the parent radical cation. In all cases, the ground state radical presents a double-occupied *p*σ orbital (and thus a long-range repulsive interaction) towards an H atom approaching from long $R_{N–H}$ distances. Table 1 shows a net decrease in parent ionization energy with increasing complexity (*i.e.* on moving from (a) to (g) in fig. 1) which, via Koopmans'-like arguments, implies an energetic lowering of (at least the shorter range part of) the dissociative ^{1}πσ* state potential.

Solvating these systems with water is shown to have only a minor effect on the energetics of N–H bond fission, and allows extension of such modelling to yet more complex systems like a model DNA-duplex. Does the increased complexity and aqueous solvation enable such 'gas-phase like' N–H bond fission in a solvated DNA-duplex when excited at λ = 266 nm (equivalent to a photon energy of 4.66 eV)? This is still not clear. Noting the present overestimation of the vertical excitation energies of bare adenine (fig. 4), there is little doubt that the duplex will absorb at this wavelength, but this alone is insufficient to assess the likelihood of photoinduced N–H bond fission via the πσ* state PES. But the studies of Markovitsi and co-workers hint at a similar, though subtly different, πσ* state mediated mechanism.[43] Following Domcke and Sobolewski,[45] the present study encourages the view that photoexcitation could promote an electron from an Ade-centred π-orbital to a σ*-orbital on an O–H bond of an H_2O molecule with which the duplex is complexed. This σ*←π excitation would yield the (observed) parent radical-cation. The subsequent release of a proton from the non-hydrogen-bonded N6′–H site would then yield the radical – a process that Table 1 confirms as being exothermic. Is this process energetically feasible at the excitation wavelength used in the experiments of Markovitsi and co-workers? Again, the present calculations are not sufficient to confirm or refute this suggestion, but both Franck-Condon effects and electron

solvation will surely lower the threshold energy for such charge transfer well below the vertical ionization energy of the duplex reported in Table 1. This re-emphasis of the potential involvement of such long range photoinduced $\sigma^* \leftarrow \pi$ electron transfers in solvated biological systems should encourage further consideration of the roles of parent radical-cations (and the radicals formed by subsequent X–H bond fission) when photoexciting heteroatom containing biomolecules in aqueous solution.

Notes

The authors declare no competing financial interest

Acknowledgements

TNVK and MNRA are grateful to the EPSRC for funding (Programme Grant: EP/L005913/1). BM gratefully acknowledges the European Union for the award of a Marie Curie International Post-Doctoral Fellowship *via* the Horizon 2020 PhARRAO initiative (grant number: 746593).

References

[1] M.N.R. Ashfold, B. Cronin, A.L. Devine, R.N. Dixon, M.G.D. Nix, The role of pisigma* excited states in the photodissociation of heteroaromatic molecules., Science. 312 (2006) 1637–40. doi:10.1126/science.1125436.

[2] A.L. Sobolewski, W. Domcke, C. Dedonder-Lardeux, C. Jouvet, Excited-state hydrogen detachment and hydrogen transfer driven by repulsive 1πσ* states: A new paradigm for nonradiative decay in aromatic biomolecules, Phys. Chem. Chem. Phys. 4 (2002) 1093–1100. doi:10.1039/b110941n.

[3] M.N.R. Ashfold, G.A. King, D. Murdock, M.G.D. Nix, T.A.A. Oliver, A.G. Sage, πσ* excited states in molecular photochemistry, Phys. Chem. Chem. Phys. 12 (2010) 1218–1238. doi:10.1039/B921706A.

[4] G.M. Roberts, V.G. Stavros, The role of πσ* states in the photochemistry of heteroaromatic biomolecules and their subunits: insights from gas-phase femtosecond spectroscopy, Chem. Sci. 5 (2014) 1698. doi:10.1039/c3sc53175a.

[5] M.G.D. Nix, A.L. Devine, B. Cronin, R.N. Dixon, M.N.R. Ashfold, High resolution photofragment translational spectroscopy studies of the near ultraviolet photolysis of phenol, J. Chem. Phys. 125 (2006) 133318. doi:10.1063/1.2353818.

[6] A. Iqbal, L.-J. Pegg, V.G. Stavros, Direct versus Indirect H Atom Elimination from Photoexcited Phenol Molecules, J. Phys. Chem. A. 112 (2008) 9531–9534. doi:10.1021/jp802155b.

[7] A.L. Devine, M.G.D. Nix, R.N. Dixon, M.N.R. Ashfold, Near-Ultraviolet Photodissociation of Thiophenol, J. Phys. Chem. A. 112 (2008) 9563–9574. doi:10.1021/jp802019v.

[8] S.G. Ramesh, W. Domcke, A multi-sheeted three-dimensional potential-energy surface for the H-atom photodissociation of phenol, Faraday Discuss. 163 (2013) 73. doi:10.1039/c3fd00006k.

[9] K. Rajak, A. Ghosh, S. Mahapatra, Photophysics of phenol and pentafluorophenol: The role of nonadiabaticity in the optical transition to the lowest bright $^1\pi\pi^*$ state, J. Chem. Phys. 148 (2018) 054301. doi:10.1063/1.5015986.

[10] Z. Lan, W. Domcke, V. Vallet, A.L. Sobolewski, S. Mahapatra, Time-dependent quantum wave-packet description of the1πσ* photochemistry of phenol, J. Chem. Phys. 122 (2005) 224315-13. doi:10.1063/1.1906218.

[11] T.N. V. Karsili, A.M. Wenge, B. Marchetti, M.N.R. Ashfold, Symmetry matters: photodissociation dynamics of symmetrically versus asymmetrically substituted phenols, Phys. Chem. Chem. Phys. 16 (2014) 588-598. doi:10.1039/C3CP53450B.

[12] M.G.D. Nix, A.L. Devine, B. Cronin, M.N.R. Ashfold, High resolution photofragment translational spectroscopy of the near UV photolysis of indole: Dissociation via the 1[small pi][sigma]* state, Phys. Chem. Chem. Phys. 8 (2006) 2610–2618. doi:10.1039/B603499C.

[13] A. Iqbal, V.G. Stavros, Exploring the Time Scales of H-Atom Elimination from Photoexcited Indole, J. Phys. Chem. A. 114 (2010) 68–72. doi:10.1021/jp908195k.

[14] B. Cronin, M.G.D. Nix, R.H. Qadiri, M.N.R. Ashfold, High resolution photofragment translational spectroscopy studies of the near ultraviolet photolysis of pyrrole, Phys. Chem. Chem. Phys. 6 (2004) 5031–5041. doi:10.1039/B411589A.

[15] G.M. Roberts, C.A. Williams, H. Yu, A.S. Chatterley, J.D. Young, S. Ullrich, V.G. Stavros, Probing ultrafast dynamics in photoexcited pyrrole: timescales for 1[small pi][sigma]* mediated H-atom elimination, Faraday Discuss. 163 (2013) 95–116. doi:10.1039/C2FD20140B.

[16] W. Xie, W. Domcke, S.C. Farantos, S.Y. Grebenshchikov, State-specific tunneling lifetimes from classical trajectories: H-atom dissociation in electronically excited pyrrole, J. Chem. Phys. 144 (2016) 104105. doi:10.1063/1.4943214.

[17] W. Credo Chung, Z. Lan, Y. Ohtsuki, N. Shimakura, W. Domcke, Y. Fujimura, Conical intersections involving the dissociative 1pisigma* state in 9H-adenine: a quantum chemical ab initio study., Phys. Chem. Chem. Phys. 9 (2007) 2075–84. doi:10.1039/b618745e.

[18] M.G.D. Nix, A.L. Devine, B. Cronin, M.N.R. Ashfold, Ultraviolet photolysis of adenine: Dissociation via the $\pi 1\sigma^*$ state, J. Chem. Phys. 126 (2007) 124312. doi:10.1063/1.2712843.

[19] S. Perun, A. L. Sobolewski, W. Domcke, Ab Initio Studies on the Radiationless Decay Mechanisms of the Lowest Excited Singlet States of 9H-Adenine, J. Am. Chem. Soc. 127 (2005) 6257-6265. doi:10.1021/JA044321C.

[20] V.B. Delchev, A.L. Sobolewski, W. Domcke, Comparison of the non-radiative decay mechanisms of 4-pyrimidinone and uracil: an ab initio study, Phys. Chem. Chem. Phys. 12

(2010) 5007–5015. doi:10.1039/B922505F.

[21] S. Perun, A.L. Sobolewski, W. Domcke, Conical Intersections in Thymine, J. Phys. Chem. A. 110 (2006) 13238–13244. doi:10.1021/jp0633897.

[22] S. Yamazaki, W. Domcke, A.L. Sobolewski, Nonradiative Decay Mechanisms of the Biologically Relevant Tautomer of Guanine, J. Phys. Chem. A. 112 (2008) 11965–11968. doi:10.1021/jp806622m.

[23] D.A. Blank, S.W. North, Y.T. Lee, The ultraviolet photodissociation dynamics of pyrrole, Chem. Phys. 187 (1994) 35–47. doi:https://doi.org/10.1016/0301-0104(94)00230-4.

[24] D. V Makhov, K. Saita, T.J. Martinez, D. V Shalashilin, Ab initio multiple cloning simulations of pyrrole photodissociation: TKER spectra and velocity map imaging, Phys. Chem. Chem. Phys. 17 (2015) 3316–3325. doi:10.1039/C4CP04571H.

[25] R. Bersohn, U. Even, J. Jortner, J. Chem. Phys. 80 (1984) 1050–1058.

[26] G.A. Bickel, D.R. Demmer, E.A. Outhouse, S.C. Wallace,, J. Chem. Phys. 91 (1989) 6013–6019.

[27] C. Plutzer, E. Nir, M.S. de Vries, K. Kleinermanns, IR-UV double-resonance spectroscopy of the nucleobase adenine, Phys. Chem. Chem. Phys. 3 (2001) 5466–5469. doi:10.1039/B107997B.

[28] S. Ullrich, N.L. Evans, H. Yu, A.N. Brouillette, The Photoprotective Properties of Adenine: Time-Resolved Photoelectron Spectroscopy at Different Excitation Wavelengths, in: Int. Conf. Ultrafast Phenom., Optical Society of America, 2010: p. WB7. doi:10.1364/UP.2010.WB7.

[29] M. Barbatti, A.C. Borin, S. Ullrich, Photoinduced processes in nucleic acids, Top. Curr. Chem. 355 (2015) 1-32. doi:10.1007/128_2014_569.

[30] B. Marchetti, T.N. V. Karsili, M.N.R. Ashfold, W. Domcke, A “bottom up”, ab initio computational approach to understanding fundamental photophysical processes in nitrogen containing heterocycles, DNA bases and base pairs, Phys. Chem. Chem. Phys. 18 (2016) 20007–20027. doi:10.1039/C6CP00165C.

[31] R. Improta, F. Santoro, L. Blancafort, Quantum Mechanical Studies on the Photophysics and the Photochemistry of Nucleic Acids and Nucleobases, Chem. Rev. 116 (2016) 3540–3593. doi:10.1021/acs.chemrev.5b00444.

[32] S. Perun, A.L. Sobolewski, W. Domcke, Photostability of 9H-adenine: mechanisms of the

radiationless deactivation of the lowest excited singlet states, Chem. Phys. 313 (2005) 107–112. doi:10.1016/J.CHEMPHYS.2005.01.005.

[33] W. Domcke, D.R. Yarkony, H. Koeppel, Conical Intersections: Theory, Computation and Experiment, 2011.

[34] W. Domcke, D.R. Yarkony, H. Koeppel, Conical Intersections: Electronic Structure, Dynamics & Spectroscopy, 2004.

[35] S. Boldissar, M.S. de Vries, How nature covers its bases, Phys. Chem. Chem. Phys. 20 (2018) 9701–9716. doi:10.1039/C8CP01236A.

[36] A.A. Beckstead, Y. Zhang, M.S. de Vries, B. Kohler, Life in the light: nucleic acid photoproperties as a legacy of chemical evolution, Phys. Chem. Chem. Phys. 18 (2016) 24228–24238. doi:10.1039/C6CP04230A.

[37] L.A. Baker, B. Marchetti, T.N. V Karsili, V.G. Stavros, M.N.R. Ashfold, Photoprotection: extending lessons learned from studying natural sunscreens to the design of artificial sunscreen constituents, Chem. Soc. Rev. 46 (2017) 3770–3791. doi:10.1039/C7CS00102A.

[38] R.P. Sinha, D.-P. Hader, UV-induced DNA damage and repair: a review, Photochem. Photobiol. Sci. 1 (2002) 225–236. doi:10.1039/B201230H.

[39] C.T. Middleton, K. de La Harpe, C. Su, Y.K. Law, C.E. Crespo-Hernández, B. Kohler, DNA Excited-State Dynamics: From Single Bases to the Double Helix, Annu. Rev. Phys. Chem. 60 (2009) 217–239. doi:10.1146/annurev.physchem.59.032607.093719.

[40] M.J. Peak, J.G. Peak, Effects of solar ultraviolet photons on mammalian cell DNA. [UVA (320-400 nm):a2], in: United States, 1991. http://www.osti.gov/scitech/servlets/purl/6106470.

[41] C.E. Crespo-Hernández, B. Cohen, P.M. Hare, B. Kohler, Ultrafast Excited-State Dynamics in Nucleic Acids, Chem. Rev. 104 (2004) 1977–2020. doi:10.1021/cr0206770.

[42] M. Gomez-Mendoza, A. Banyasz, T. Douki, D. Markovitsi, J.-L. Ravanat, Direct Oxidative Damage of Naked DNA Generated upon Absorption of UV Radiation by Nucleobases, J. Phys. Chem. Lett. 7 (2016) 3945–3948. doi:10.1021/acs.jpclett.6b01781.

[43] A. Banyasz, T. Ketola, L. Martinez-Fernandez, R. Improta, D. Markovitsi, Adenine radicals generated in alternating AT duplexes by direct absorption of low-energy UV radiation, Faraday Discuss. 207 (2018) 181–197. doi:10.1039/C7FD00179G.

[44] A. Banyasz, L. Martínez-Fernández, C. Balty, M. Perron, T. Douki, R. Improta, D. Markovitsi, Absorption of Low-Energy UV Radiation by Human Telomere G-Quadruplexes Generates Long-Lived Guanine Radical Cations, J. Am. Chem. Soc. 139 (2017) 10561–10568. doi:10.1021/jacs.7b05931.

[45] A.L. Sobolewski, W. Domcke, Photoinduced electron and proton transfer in phenol and its clusters with water and ammonia, J. Phys. Chem. A. 105 (2001) 9275–9283. doi:10.1021/jp011260l.

[46] O.P.J. Vieuxmaire, Z. Lan, A.L. Sobolewski, W. Domcke, *Ab initio* characterization of the conical intersections involved in the photochemistry of phenol, J. Chem. Phys. 129 (2008) 224307. doi:10.1063/1.3028049.

[47] P. Goyal, C.A. Schwerdtfeger, A. V. Soudackov, S. Hammes-Schiffer, Proton Quantization and Vibrational Relaxation in Nonadiabatic Dynamics of Photoinduced Proton-Coupled Electron Transfer in a Solvated Phenol-Amine Complex, J. Phys. Chem. B. 120 (2016). doi:10.1021/acs.jpcb.5b12015.

[48] J.W. Riley, B. Wang, J.L. Woodhouse, M. Assmann, G.A. Worth, H.H. Fielding, Unravelling the Role of an Aqueous Environment on the Electronic Structure and Ionization of Phenol Using Photoelectron Spectroscopy, J. Phys. Chem. Lett. 9 (2018) 678–682. doi:10.1021/acs.jpclett.7b03310.

[49] T.A.A. Oliver, Y. Zhang, A. Roy, M.N.R. Ashfold, S.E. Bradforth, Exploring Autoionization and Photoinduced Proton-Coupled Electron Transfer Pathways of Phenol in Aqueous Solution, J. Phys. Chem. Lett. 6 (2015) 4159–4164. doi:10.1021/acs.jpclett.5b01861.

[50] M.J. Frisch, G.W. Trucks, H.B. Schlegel, G.E. Scuseria, M.A. Robb, J.R. Cheeseman, G. Scalmani, V. Barone, B. Mennucci, G.A. Petersson, H. Nakatsuji, M. Caricato, X. Li, H.P. Hratchian, A.F. Izmaylov, J. Bloino, G. Zheng, J.L. Sonnenberg, M. Hada, M. Ehara, K. Toyota, R. Fukuda, J. Hasegawa, M. Ishida, T. Nakajima, Y. Honda, O. Kitao, H. Nakai, T. Vreven, J.A. Montgomery, J.E. Peralta, F. Ogliaro, M. Bearpark, J.J. Heyd, E. Brothers, K.N. Kudin, V.N. Staroverov, R. Kobayashi, J. Normand, K. Raghavachari, A. Rendell, J.C. Burant, S.S. Iyengar, J. Tomasi, M. Cossi, N. Rega, J.M. Millam, M. Klene, J.E. Knox, J.B. Cross, V. Bakken, C. Adamo, J. Jaramillo, R. Gomperts, R.E. Stratmann, O. Yazyev, A.J. Austin, R. Cammi, C. Pomelli, J.W. Ochterski, R.L. Martin, K. Morokuma,

V.G. Zakrzewski, G.A. Voth, P. Salvador, J.J. Dannenberg, S. Dapprich, A.D. Daniels, Farkas, J.B. Foresman, J. V Ortiz, J. Cioslowski, D.J. Fox, Gaussian 09, Revision B.01, Gaussian 09, Revis. B.01, Gaussian, Inc., Wallingford CT. (2009).

[51] J.-D. Chai, M. Head-Gordon, Long-range corrected hybrid density functionals with damped atom-atom dispersion corrections, Phys. Chem. Chem. Phys. 10 (2008) 6615–6620. doi:10.1039/B810189B.

[52] W.J. Hehre, R. Ditchfield, R.F. Stewart, J.A. Pople, Self-Consistent Molecular Orbital Methods. IV. Use of Gaussian Expansions of Slater-Type Orbitals. Extension to Second-Row Molecules, J. Chem. Phys. 52 (1970) 2769–2773. doi:10.1063/1.1673374.

[53] S. Dapprich, I. Komáromi, K.S. Byun, K. Morokuma, M.J. Frisch, A new ONIOM implementation in Gaussian98. Part I. The calculation of energies, gradients, vibrational frequencies and electric field derivatives, J. Mol. Struct. THEOCHEM. 461–462 (1999) 1–21. doi:https://doi.org/10.1016/S0166-1280(98)00475-8.

[54] A. Ernst, K. Rainer, F. Peter, Optimization and application of lithium parameters for PM3, J. Comput. Chem. 14 (2004) 1301–1312. doi:10.1002/jcc.540141106.

[55] A.J. Pepino, J. Segarra-Martí, A. Nenov, R. Improta, M. Garavelli, Resolving Ultrafast Photoinduced Deactivations in Water-Solvated Pyrimidine Nucleosides, J. Phys. Chem. Lett. 8 (2017) 1777-1783. doi:10.1021/acs.jpclett.7b00316.

[56] R. Salomon-Ferrer, D.A. Case, R.C. Walker, An overview of the Amber biomolecular simulation package, Wiley Interdiscip. Rev. Comput. Mol. Sci. 3 (2013) 198–210. doi:10.1002/wcms.1121.

[57] L. Martínez, R. Andrade, E.G. Birgin, J.M. Martínez, PACKMOL: A package for building initial configurations for molecular dynamics simulations, J. Comput. Chem. 30 (2009) 2157–2164. doi:10.1002/jcc.21224.

[58] H. Reisler, A.I. Krylov, Interacting Rydberg and valence states in radicals and molecules: experimental and theoretical studies, Int. Rev. Phys. Chem. 28 (2009) 267–308. doi:10.1080/01442350902989170.

[59] S. Perun, A.L. Sobolewski, W. Domcke, Role of electron-driven proton-transfer processes in the excited-state deactivation of the adenine-thymine base pair, J. Phys. Chem. A. 110 (2006) 9031–9038. doi:10.1021/jp061945r.

[60] L.B. Clark, G.G. Peschel, I. Tinoco, Vapor Spectra and Heats of Vaporization of Some

Purine and Pyrimidine Bases1, J. Phys. Chem. 69 (1965) 3615–3618. doi:10.1021/j100894a063.

[61] N. Joon Kim, H. Kang, Y. Dong Park, S. Keun Kim, Dispersed fluorescence spectroscopy of jet-cooled adenine, Phys. Chem. Chem. Phys. 6 (2004) 2802–2805. doi:10.1039/B313467A.